Journal of Biomolecular NMR, **23:** 303–309, 2002.
KLUWER/ESCOM

An NMR method for studying the kinetics of metal exchange in biomolecular systems

Renato Barbieri[a], P.J. Hore[b], Claudio Luchinat[c,*] & Roberta Pierattelli[a]
[a]*Department of Chemistry and Magnetic Resonance Center and* [c]*Department of Agricultural Biotechnology and Magnetic Resonance Center, University of Florence, 50019 Sesto Fiorentino (Florence), Italy;* [b]*Oxford Centre for Molecular Sciences, Physical and Theoretical Chemistry Laboratory, Oxford University, Oxford OX1 3QZ, UK*

Received 3 June 2002; Accepted 18 July 2002

Abstract

The kinetics of lanthanide (III) exchange for calcium(II) in the C-terminal EF-hand of the protein calbindin D_{9k} have been studied by one-dimensional (1D) stopped-flow NMR. By choosing a paramagnetic lanthanide (Ce^{3+}), kinetics in the sub-second range can be easily measured. This is made possible by the fact that (i) the kinetic behaviour of hyperfine shifted signals can be monitored in 1D NMR and (ii) fast repetition rates can be employed because these hyperfine shifted signals relax fast. It is found that the Ce^{3+}-Ca^{2+} exchange process indeed takes place on a sub-second timescale and can be easily monitored with this technique. As the rate of calcium-cerium substitution was found not to depend on the presence of excess calcium in solution, the kinetics of the process were interpreted in terms of a bimolecular associative mechanism, and the rate constants extracted. Interestingly, the dissociative mechanism involving the *apo* form of the protein, which is generally assumed for metal ion exchange at protein binding sites, was not in agreement with our data.

Introduction

The presence of paramagnetic centres in an NMR sample, either as free ions or bound to solute molecules, often causes difficulties when recording high quality NMR spectra. However, there are a number of cases in which this situation can be turned to advantage. For instance, paramagnetic lanthanide ions have long been used to enhance the resolution of crowded NMR spectra through their ability to shift the signals of nuclear spins close to the metal center (Kurland and McGarvey, 1970; Bleaney, 1972). To a first approximation, for nuclei that do not exhibit a Fermi contact interaction with the electron spin, the size of the chemical shift is proportional to the reciprocal of the third power of the nucleus-metal distance (Bleaney, 1972; Bertini and Luchinat, 1996). Recently, these effects have been used to obtain long-range geometrical information on the structure of diamagnetic metalloproteins in which a diamagnetic metal (e.g., a calcium ion) had been substituted with a paramagnetic lanthanide (Bentrop et al., 1997; Contreras et al., 1999; Allegrozzi et al., 2000; Bertini et al., 2001). It has been shown that careful choice of the lanthanide ion allows different regions of a protein to be monitored, even by means of simple one-dimensional (1D) NMR experiments (Allegrozzi et al., 2000; Bertini et al., 2001). We show here that these 'paramagnetic peaks' can be conveniently used as a probe to monitor the kinetics of metal-ion exchange.

The use of NMR to study reactions of proteins in *real time* started nearly 30 years ago, with the aim of understanding enzyme mechanisms (Grimaldi et al., 1972; Grimaldi and Sykes, 1975). Since that time a variety of (mostly spectroscopic) real-time techniques have been developed to investigate the thermodynamics and kinetics of protein folding and unfolding (Van Nuland et al., 1998; Kaptein et al., 1978; Kaptein, 1978). Procedures involving rapid mixing within the NMR sample tube are now being devised (Balbach et al., 1995; Baum and Brodsky, 1997; Hore et al., 1997; Hoeltzli and Frieden, 1998; Hamang et al.,

*To whom correspondence should be addressed.
E-mail: luchinat@cerm.unifi.it

2000; Kuhn and Schwalbe, 2000; Wirmer et al., 2001) that are beginning to transform NMR into a general and powerful technique for studying a wide range of fundamental events in folding-unfolding processes on the 100 ms – 1 s timescale, at the level of individual amino acid residues. Even though the field is undergoing continuous development, mainly with the aim of both retaining the wealth of structural information usually afforded by high-resolution protein NMR and improving the time resolution of the measurements, a trade-off between the two is often unavoidable.

Metal binding or metal exchange processes are usually fast and thus need measurements in the range of stopped-flow techniques (Van Nuland et al., 1998). The requirement for rapid acquisition of NMR data usually compromises the spectral resolution and so can restrict the possibility of monitoring events at the level of single residues and analysing their time-dependence. The task can however still be tackled if nuclei in the region of the protein where exchange takes place give rise to signals that are well resolved in the NMR spectrum. In addition, the paramagnetic contribution to nuclear spin relaxation rates, which can be extremely large, makes it possible to acquire free induction decays at high repetition rates. As mentioned above, this is the case when lanthanides are the exchanging metals because of the paramagnetic-induced shifts of resonances to otherwise empty spectral regions.

Ion binding to metalloproteins is a complicated process involving a number of phenomena. For instance, in calcium-binding proteins made up of EF-hand domains (usually two EF-hands per domain), the following factors all influence the overall rate constant: the rate at which a calcium ion (or another cation, such as a lanthanide) loses one water molecule from its hydration shell, its interactions with charged residues on the protein surface (even at positions remote from the actual binding site), the hydrophobic packing of the domain, the occupancy state of the other EF-hand in the domain, and the strength of hydrogen bonds from the protein to the bound Ca^{2+} coordinating water (Corson et al., 1983a; Vogel et al., 1985; Martin et al., 1990; Kragelund et al., 1998; Fast et al., 2001). However, despite this complexity, a simple first-order kinetic mechanism is found to be valid for ion release in presence of a (fast) competitive chelator. The same mechanism (i.e., dissociative) is usually assumed when one metal ion is exchanged for another, i.e., metal exchange takes place in a two-step process involving the protein in its *apo* form (Corson et al., 1983b; Breen et al., 1985; Buccigross et al., 1986). However, not all the experimental data seem to be in agreement with this assumption and, at least in one case, an additional, bimolecular, associative mechanism, involving a rapid equilibrium between the competing metal ion and a 'subsidiary' binding site on the protein, has been invoked (Breen et al., 1985).

In order to check whether the associative mechanism is a reasonable alternative to the dissociative one, we have measured the rates of lanthanide-calcium substitution in the calcium binding protein calbindin D_{9k} (also known as ICaBP, Intestinal Calcium Binding Protein) using 1D stopped-flow NMR. This protein, in the presence of stoichiometric amounts of calcium, readily binds two metal ions through EF-hand motifs (although under physiologically relevant conditions a magnesium ion may replace one of the calcium ions (Andersson et al., 1997)). The C-terminal calcium-binding site has a much higher relative lanthanide/calcium affinity than the N-terminal site (Vogel et al., 1985; Linse et al., 1987; Akke et al., 1991); thus a complete and selective metal substitution is readily achieved by titration of the Ca^{2+}-loaded form of the protein with one equivalent of lanthanide, the relative affinity of this binding site being about 2 orders of magnitude higher than that of the N-terminal pseudo EF-hand (Shelling et al., 1985; Hofmann et al., 1988). Though lanthanide ions have a higher charge and different geometrical requirements for coordination with respect to calcium, the substitution into the C-terminal EF-hand causes no major change in the three-dimensional structure (Dorrington et al., 1978; Shelling et al., 1985). Both the fully calcium-loaded (CaCaCb) and the cerium monosubstituted (CaCeCb) forms of the protein have been extensively characterized (Allegrozzi et al., 2000). We demonstrate here that the process takes place on a sub-second timescale that is easily accessible with the experimental approach presented. Our results shed light on the rate-limiting step of the reaction, indicating that a concerted process is more likely than a sequence of reactions involving an *apo* form of the protein that rapidly binds cerium. Aside from the intrinsic interest in metal ion exchange processes, the ability to follow the growth of 'paramagnetic peaks' upon calcium-lanthanide substitution makes it feasible to study other dynamic processes involving structural changes of proteins which could not be otherwise be observed because of poor spectral resolution.

Materials and methods

Materials

The fully-loaded calcium form of the P43M mutant of bovine calbindin D_{9k} was used for the experiments. This mutant was preferred to the wild-type protein to avoid the cis/trans isomerization affecting the native protein at position 43. The expression and purification of this protein has been described elsewhere (Brodin et al., 1986; Johansson et al., 1990); the expression system was a generous gift of Prof. S. Forsén. A 2.75 mM solution of the protein was prepared in unbuffered D_2O and the pH adjusted to 6.4 (uncorrected for the isotope effect). Di-ethylenetriaminepentaacetic acid (DTPA, Acros Inc.) and $CeCl_3$ were used as solutions in D_2O, at a pH of 6.4.

Equipment

The fast injection device, especially designed to deliver small volumes (tens of microliters) of liquids rapidly into an NMR tube in the spectrometer probehead, is described elsewhere (Balbach et al., 1995; Maeda et al., 2000). The injection was triggered by voltage-gating pulses (typical duration: 20–40 ms) in the NMR pulse sequence, which consisted of a standard pulse-acquisition scheme modified to provide an array of single-scan experiments as a data set. One hundred single-scan spectra were acquired prior to the injection (in order to ensure steady-state conditions), followed by the trigger pulse to drive the injection, and the acquisition of a further 800 single-scan spectra. The repetition time was kept constant throughout the whole experiment and ranged from 38 to 57 ms, depending on the length of the injection trigger pulse. The experiments were carried out with either a hard 90° pulse or a 'jump-and-return' pulse (Hore, 1983) (to avoid exciting the residual HDO signal) as the detection pulse, acquiring 1024 data points over a 48 000 Hz spectral width with a 1 bit oversampling of the acquired data. The injected volume was 70 µl. The spectrometer used was a Bruker AVANCE 600, with a resonating frequency of 600.13 MHz for protons, equipped with a high-power proton-selective probe.

Data analysis

The signal intensities as a function of time were fitted initially to the expression

$$I(t) = I_0[1 - e^{-k_{\mathrm{obs}}(t-t_0)}]$$

and later to

$$I(t) = I_0\overline{xx'}\frac{e^{(\bar{x}'-x)(k_f-k_r)(t-t_0)} - 1}{\bar{x}'e^{(\bar{x}'-x)(k_f-k_r)(t-t_0)} - \bar{x}},$$

where x is the concentration of CaCeCb at time t, $\bar{x}$ is its equilibrium value, $\bar{x}'$ is given by $\bar{x}' = (K-1)^{-1} \cdot \{K([\mathrm{Ce}]_0+[\mathrm{CaCeCb}]_0)+[\mathrm{Ca}]_0+[\mathrm{CaCeCb}]_0\}-\bar{x}$, $k_{f,r}$ are the forward and reverse rate constants for the associative mechanism (Equation 2 below), respectively, and $K(= k_f/k_r)$ is the equilibrium constant for the exchange reaction (Emanuel' and Knorre, 1973). t_0 is an offset value for the time axis, which was kept fixed (see below and in Results). The fitting was carried out by a home-written Matlab routine (The Mathworks Inc.) using a Levenberg–Marquardt non-linear least-squares fitting algorithm (Marquardt, 1963). The errors quoted for the rate constants, k, were calculated by assuming that all the intensities are affected by the same statistical error, and validated through a Monte Carlo analysis based upon 500 synthetic datasets. The time $t = 0$ corresponds to the rising edge of the excitation pulse immediately following the mixing, while t_0 was kept fixed at 54 ms (as calculated from a 'calibration' experiment – see Results). Making t_0 adjustable gave no statistically significant difference in the results.

Results

To assess the ability of the technique to observe NMR intensity changes via single-scan spectra acquired at a very high repetition rate, we followed the uptake of Ce^{3+} by DTPA, a multidentate chelator known to form soluble, highly stable, chemically inert 1:1 complexes with lanthanide ions and which shows well resolved hyperfine shifted resonances in its 1D NMR spectrum (Jenkins and Lauffer, 1988). A stoichiometric amount of aqueous $CeCl_3$ (70 µl) was injected into 430 µl of a 12 mM solution of the ligand in the presence of excess calcium in the NMR tube at pH 6.4, as described above. As expected, the formation of the cerium complex was very fast; the new paramagnetically shifted resonances grew to their full intensity within a few time points as shown in Figure 1. The rate constant of the single exponential growth curve is $19 \pm 2\ \mathrm{s}^{-1}$. Since the kinetic constant for the complexation reaction is known to occur on a much shorter timescale ($10 \times 10^8\ \mathrm{s}^{-1}$) (Corson et al., 1983), the measured value almost certainly reflects the time needed to complete the injection and mixing. The reciprocal of this

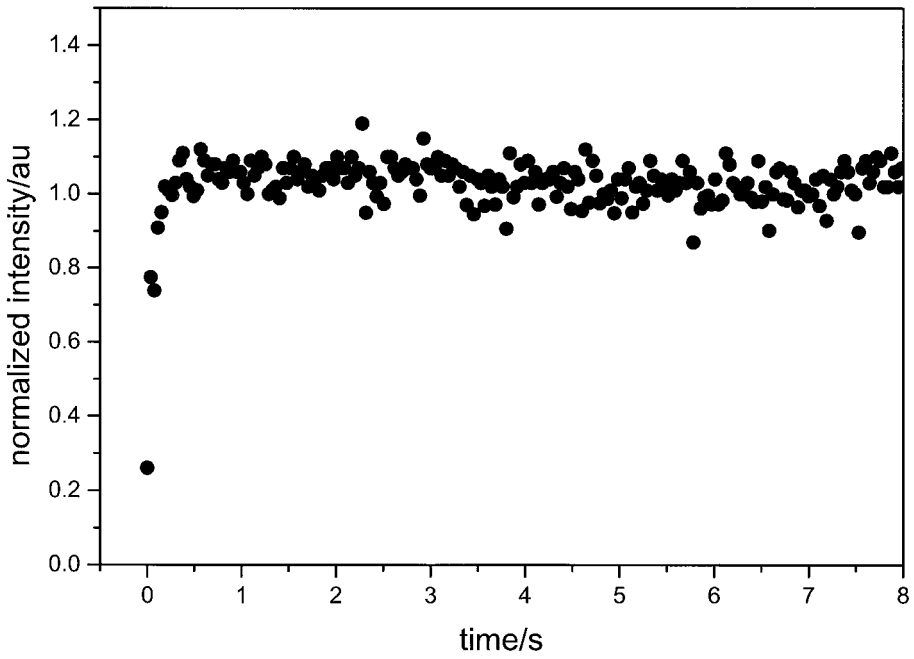

Figure 1. Time course of the metal ion substitution: $Ca^{2+}DTPA + Ce^{3+} \rightarrow Ce^{3+}DTPA + Ca^{2+}$, as monitored by the variation in intensity of the hyperfine-shifted DTPA resonance at −7.3 ppm. The intensities measured before the injection are omitted.

Table 1. Empirical rate constants calculated by fitting experimental signal intensities to a single exponential growth function

Proton	k_{obs}/s^{-1} no excess Ca^{2+}	k_{obs}/s^{-1} excess Ca^{2+}
HN E60	1.21 ± 0.24	1.42 ± 0.28
HN D58	1.13 ± 0.22	1.28 ± 0.34
HG1 61	1.52 ± 0.42	1.31 ± 0.24
HG2 V61	1.23 ± 0.26	1.14 ± 0.20
NH2 N56	1.15 ± 0.28	1.02 ± 0.22
HA V61	1.08 ± 0.22	0.82 ± 0.22

value (54 ms) was thus chosen as the (fixed) time offset, t_0, for the subsequent fittings (see Materials and methods).

We then measured the rate of the metal-exchange reaction for calbindin D_{9k}. A 2.75 mM sample of CaCaCb in D_2O was rapidly mixed with a stoichiometric amount of aqueous $CeCl_3$ (injected into the NMR tube) and the intensities of the hyperfine-shifted resonances were monitored. The assigned NMR spectrum of the fully substituted CaCeCb is displayed in Figure 2.

Although the signal-to-noise ratio of the single-scan spectra acquired at intervals of ∼40 ms is rather poor (see inset in Figure 2), the growth of the paramagnetic signals can still be recorded even for resonances close to the diamagnetic region of the NMR spectrum. In Figure 3, we show, as an example, the build-up curve for the γ_2 methyl group of Val 61 resonating at −3.7 ppm. The time constants for the growth curves, assumed to be mono-exponential, of the detectable resonances are reported in the second column of Table 1. Their values, which are affected by rather high uncertainties, do not differ outside the experimental error, thus indicating that the protons are affected by the presence of the lanthanide ion in much the same way. This, in turn, rules out the presence of an intermediate species with a lifetime of hundreds of milliseconds during the exchange reaction.

The experiment was then repeated under identical conditions except that a 10-fold excess of calcium was used to check for any influence of the CaCaCb $\rightleftarrows$ Ca + CaECb equilibrium on the rate of Ce^{3+} uptake (CaECb stands for calbindin D_{9k} with the C-terminal EF-hand empty). The relevant rate constants, assuming a mono-exponential growth, are reported in the third column of Table 1. Within experimental error, the time constants measured with a ten-fold excess

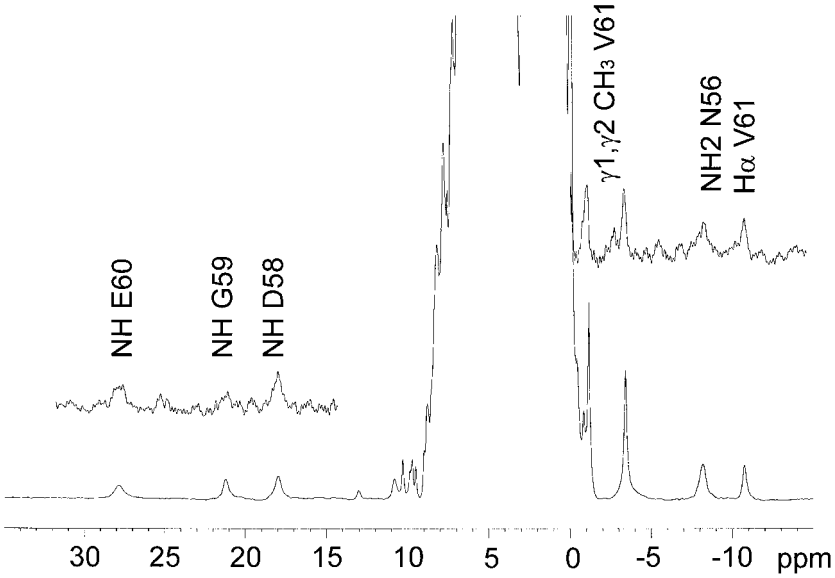

Figure 2. ^{1}H NMR spectrum of CaCeCb recorded at 600 MHz. Two portions of a single-scan real-time trace are shown in the inset.

of Ca^{2+} do not differ from those obtained with a stoichiometric amount of Ca^{2+}.

Discussion

The two simplest kinetic models for the metal exchange reaction are a two-step process, via an *apo* form of the protein:

$$\mathrm{CaCaCb} \rightleftarrows \mathrm{CaECb} + \mathrm{Ca}, \tag{1a}$$

$$\mathrm{CaECb} + \mathrm{Ce} \rightarrow \mathrm{CaCeCb} \tag{1b}$$

and a concerted mechanism:

$$\mathrm{CaCaCb} + \mathrm{Ce} \rightleftarrows \mathrm{CaCeCb} + \mathrm{Ca}. \tag{2}$$

The one-way arrow in Equation 1b is justified by the high affinity displayed by lanthanides towards a canonical EF-hand motif (Shelling et al., 1985). Equation 2, for generality, is considered as an equilibrium reaction, despite the ca. two-orders-of magnitude difference in the affinity of the C-terminal EF-hand in D_{9k} for Ca^{2+} and Ce^{3+} (Shelling et al., 1985; Hofmann et al., 1988).

The relevant kinetic equations are then:

$$\frac{\mathrm{d[CaCeCb]}}{\mathrm{d}t} = \frac{k_{\mathrm{off}}^{\mathrm{Ca}} k_{\mathrm{on}}^{\mathrm{Ce}} [\mathrm{Ce}]_t [\mathrm{CaCaCb}]_t}{k_{\mathrm{on}}^{\mathrm{Ca}} [\mathrm{Ca}]_t + k_{\mathrm{on}}^{\mathrm{Ce}} [\mathrm{Ce}]_t} \tag{3}$$

and

$$\frac{\mathrm{d[CaCeCb]}}{\mathrm{d}t} = k_f [\mathrm{Ce}]_t [\mathrm{CaCaCb}_t - k_r [\mathrm{Ca}]_t [\mathrm{CaCeCb}]_t, \tag{4}$$

respectively, where the steady state approximation for the intermediate was used in deriving Equation 3.

The observed rate of the ion-exchange process is independent, within the experimental error, of the actual concentration of calcium. If the reaction occurs through an *apo* state (Equations 1a and 1b), as would be the case for a typical pre-equilibrium reaction, then the time constant for the formation of CaCeCb would be strongly affected by the excess concentration of Ca^{2+}, unless the relationship $k_{\mathrm{on}}^{\mathrm{Ca}}[\mathrm{Ca}]_t \ll k_{\mathrm{on}}^{\mathrm{Ce}}[\mathrm{Ce}]_t$ in Equation 3 holds. However, this does not seem to be the case, since k_{on} literature values for metals bound to EF-hands show that there are no large differences between calcium and lanthanides, and that the differences in affinity constants are principally determined by k_{off} values (Corson et al., 1983). It thus appears that the first model is incompatible with the results presented here. The single-step associative mechanism (Equation 2) is the only simple alternative, although other more complicated models may also be consistent with the experimental data. Having ruled out the two-step (dissociative) mechanism we fitted the signal intensities to the integrated form of Equation 4 (see *Materials and methods*). As the reaction rate is dependent on the equilibrium constant of the exchange reaction, it was necessary to include this value in the calculations. From titration experiments of calcium-loaded calbindin D_{9k} with several lanthanides, as monitored by ^{1}H-^{15}N HSQC spectra, a K value in the order of 10^3 was estimated; by using

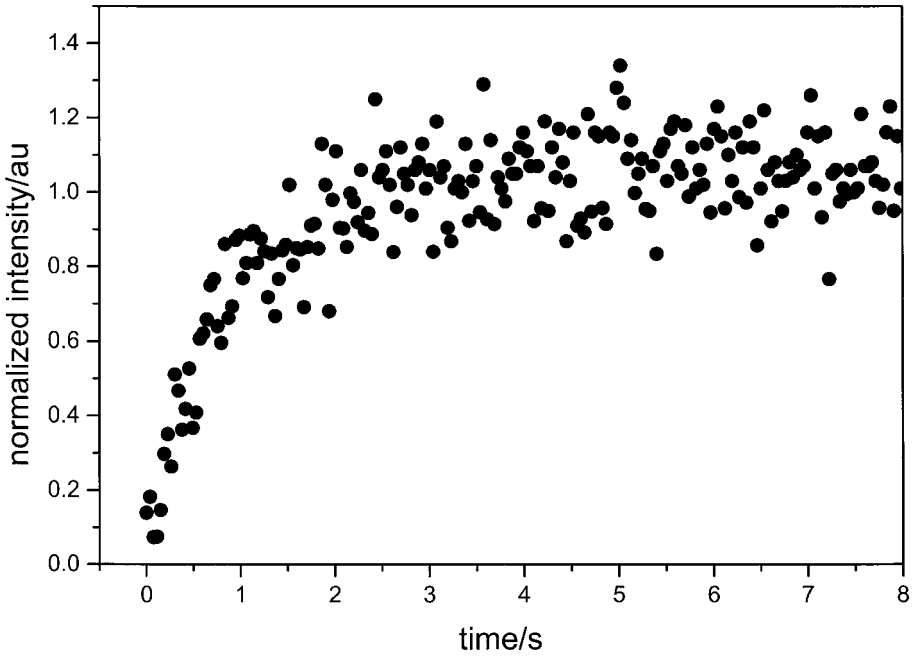

Figure 3. Time course of calcium substitution by cerium in the C-terminal EF-hand of protein calbindin D_{9k}, as monitored by change in intensity of Val 61 γ_2-CH_3 peak. The intensities measured before the injection are omitted.

this value we obtained $k_{f,r}$ values for each of the six datasets that do not differ from one another outside the experimental error. To increase the precision of the calculated rate constants, the experimental data for each set were then fitted simultaneously to single $k_{f,r}$ values, yielding $k_f = 945 \pm 64$ M^{-1} s^{-1} and $k_r = 0.95 \pm 0.06$ M^{-1} s^{-1} in the absence of excess calcium, and $k_f = 993 \pm 56$ M^{-1} s^{-1} and $k_r = 0.99 \pm 0.06$ M^{-1} s^{-1} when excess calcium was added to the reagents. The fact that the integrated form of Equation 4 correctly fits our experimental data and that the resulting rate constants are the same within the experimental error ($\sim 7\%$) proves that the associative mechanism is a realistic model to describe the kinetics of Ca-lanthanide exchange processes in EF-hands. Furthermore, the results presented here convincingly show that paramagnetic probes enable the use of standard 1D NMR experiments to monitor molecular processes on the timescale of hundred of milliseconds, such as folding/unfolding, ion binding, protein-protein interactions, etc. The technique is thus complementary to, and lies somewhat in between, already established methodologies, such as time-resolved photo-CIDNP (Hore et al., 1997; Maeda et al., 2000; Wirmer et al., 2001) and stopped-flow 2D NMR (Balbach et al., 1996; Lyon et al., 1999). The former can monitor processes as fast as 5 s^{-1}, the latter only below 0.05 s^{-1}. Of course, all these techniques are expected to experience great benefit from theever-increasing availability of high-sensitivity cryoprobes, with the advantage that the same signal-to-noise ratio could be achieved at lower protein concentrations, thus lowering reaction rates and thereby making more dynamic processes experimentally accessible.

Acknowledgements

The work has been carried out at the Research Infrastructure 'PARABIO'. The EC Access to Research Infrastructures Action of the Improving Human Potential Programme (Contract No. HPRI-CT-1999-00009) is gratefully acknowledged. This work was supported in part by the EC contract No. HPRI-CT-1999-50006 (Transient NMR). The calbindin D_{9k} expression system was a generous gift of Prof. S. Forsén.

References

Akke, M., Forsén, S. and Chazin, W.J. (1991) *J. Mol. Biol.*, **220**, 173–189.

Allegrozzi, M., Bertini, I., Janik, M.B.L., Lee, Y.-M., Liu, G. and Luchinat, C. (2000) *J. Am. Chem. Soc.*, **122**, 4154–4161.

Andersson, M., Malmendal, A., Linse, S., Ivarson, I., Forsén, S. and Svensson, L.A. (1997) *Protein Sci.*, **6**, 1139–1147.

Balbach, J., Forge, V., Lau W.S., Van Nuland, N.A.J., Brew, K. and Dobson, C.M. (1996) *Science*, **274**, 1161–1163.
Balbach, J., Forge, V., Van Nuland, N.A.J., Winder, S.L., Hore, P.J. and Dobson, C.M. (1995) *Nat. Struct. Biol.*, **2**, 865–870.
Baum, J. and Brodsky, B. (1997) *Fold. Des.*, **2**, R53–R60.
Bentrop, D., Bertini, I., Cremonini, M.A., Forsén, S., Luchinat, C. and Malmendal, A. (1997) *Biochemistry*, **36**, 11605–11618.
Bertini, I. and Luchinat, C. (1996) *NMR of Paramagnetic Substances*, 1st edn., Coord. Chem. Rev. 150, Elsevier, Amsterdam.
Bertini, I., Janik, M.B.L., Lee, Y.-M., Luchinat, C. and Rosato, A. (2001) *J. Am. Chem. Soc.*, **123**, 4181–4188.
Bleaney, B. (1972) *J. Magn. Reson.*, **8**, 91–100.
Breen, P.J., Johnson, K.A. and Horrocks, W.D.J. (1985) *Biochemistry*, **24**, 4997–5004.
Brodin, P., Grundstrom, T., Hofmann, T., Drakenberg, T., Thulin, E. and Forsén, S. (1986) *Biochemistry*, **25**, 5371–5377.
Buccigross, J.M., O'Donnell, C.L. and Nelson, D.J. (1986) *Biochem. J.*, **235**, 677–684.
Contreras, M.A., Ubach, J., Millet, O., Rizo, J. and Pons, M. (1999) *J. Am. Chem. Soc.*, **121**, 8947–8948.
Corson, D.C., Lee, L., McQuaid, G.A. and Sykes, B.D. (1983a) *Can. J. Biochem. Cell Biol.*, **61**, 860–867.
Corson, D.C., Williams, T.C. and Sykes, B.D. (1983b) *Biochemistry*, **22**, 5882–5889.
Dorrington K.J., Kells D.I.C., Hitchman A.J.W, Harrison J.E. and Hofmann, T. (1978) *Can. J. Biochem.*, **56**, 492–499.
Emanuel' N.M. and Knorre D.G. (1973) *Chemical Kinetics – Homogeneous Reactions*, Halsted Press, Jerusalem.
Fast, J., Gippert, G.P., Muranyi, A., Thulin, E., Evenäs, J., Svensson, L.A. and Linse, S. (2001) *Biochemistry*, **40**, 9887–9895.
Grimaldi, J.J. and Sykes, B.D. (1975) *Rev. Sci. Instr.*, **46**, 1201–1205.
Grimaldi, J.J., Baldo, J., McMurray, C. and Sykes, B.D. (1972) *J. Am. Chem. Soc*, **94**, 7641–7645.
Hamang M., Sanson A., Liagre L., Forge, V. and Berthault, P. (2000) *Rev. Sci. Instr.*, **71**, 2180–2183.
Hoeltzli, S.D. and Frieden, C. (1998) *Biochemistry*, **37**, 387–398.
Hofmann, T., Eng S., Lilja H., Drakenberg, T., Vogel, H.J. and Forsén, S. (1988) *Eur. J. Biochem.*, **172**, 307–313.
Hore, P.J. (1983) *J. Magn. Reson.*, **54**, 539–542.
Hore, P.J., Winder, S.L., Roberts, C.H. and Dobson, C.M. (1997) *J. Am. Chem. Soc*, **119**, 5049–5050.
Jenkins, B.G. and Lauffer, R.B. (1988) *Inorg. Chem.*, **27**, 4730–4738.
Johansson, C., Brodin, P., Grundstrom, T., Thulin, E., Forsén, S. and Drakenberg, T. (1990) *Eur. J. Biochem.*, **187**, 455–460.
Kaptein, R. (1978) In *NMR Spectroscopy in Molecular Biology*, Pullman B. (Ed.), D. Reidel Publ. Co., Dordrecht, pp. 211–229.
Kaptein, R., Dijkstra, K. and Nicolay, K. (1978) *Nature*, **274**, 293–294.
Kragelund, B.B., Jönsson, M., Bifulco, G., Chazin, W.J., Nilsson, A., Finn, B.E. and Linse, S. (1998) *Biochemistry*, **37**, 8926–8937.
Kuhn, T. and Schwalbe, H. (2000) *J. Am. Chem. Soc.*, **122**, 6169–6174.
Kurland, R.J. and McGarvey, B.R. (1970) *J. Magn. Reson.*, **2**, 286–301.
Linse, S., Brodin, P., Drakenberg, T., Thulin, E., Sellers, P., Elmden, K., Grundstrom, T. and Forsén, S. (1987) *Biochemistry*, **26**, 6723–6735.
Lyon, C.E., Jones, J.A., Redfield, C., Dobson, C.M. and Hore, P.J. (1999) *J. Am. Chem. Soc.*, **121**, 6505–6506.
Maeda, K., Lyon, C.E., Lopez, J.J., Cemazar, M., Dobson, C.M. and Hore, P.J. (2000) *J. Biomol. NMR*, **16**, 235–244.
Marquardt, D.W. (1963) *J. Soc. Ind. Appl. Math.*, **11**, 431–441.
Martin, S.R., Linse, S., Johansson, C., Bayley, P.M. and Forsén, S. (1990) *Biochemistry*, **29**, 4188–4193.
Shelling, J.G., Hofmann, T. and Sykes, B.D. (1985) *Biochemistry*, **24**, 2332–2338.
Van Nuland, N.A.J., Forge, V., Balbach, J. and Dobson, C.M. (1998) *Acc. Chem. Res.*, **31**, 773–780.
Vogel, H.J., Drakenberg, T., Forsén, S., O'Neil, J.D. and Hofmann, T. (1985) *Biochemistry*, **24**, 3870–3876.
Wirmer, J., Kuhn, J. and Schwalbe, H. (2001) *Angew. Chem. Int. Ed.*, **40**, 4248–4251.